Electronic supplementary information

All-inorganic open frameworks based on gigantic four-shell

Ln@W$_8$@Ln$_8$@(SiW$_{12}$)$_6$ clusters

Jin-Hua Liu,[a] Li-Dan Lin,[a] Guo-Qiang Wang,[b] Ling-Yun Li,[b] Yan-Qiong Sun,[a] Xin-Xiong Li,*[ac] and Shou-Tian Zheng*[a]

[a]*State Key Laboratory of Photocatalysis on Energy and Environment, College of Chemistry, Fuzhou University, Fuzhou, Fujian 350108, China.*

[b]*Collega of Materials Science and Engineering, Fuzhou University, Fuzhou, Fujian 350108, China.*

[c]*State Key Laboratory of Structural Chemistry, Fujian Institute of Research on the Structure of Matter, Chinese Academy of Science, Fuzhou, Fujian 350108, China.*

This file includes:

Section S1 Synthesis and Methods

Section S2 Additional Table

Section S3 Additional Figures

Section S4 References

Section S1 Synthesis and Methods

Materials and General methods：$Na_{10}[\alpha\text{-}SiW_9O_{34}]\cdot16H_2O$ was synthesized on the basis of literature method and proved by IR spectroscopy.[1] Other reactants and solvents were obtained from commercial sources and used for reactions without further purification. Powder XRD patterns were obtained using a RIGAKU-Miniflex II diffractometer with Cu $K\alpha$ radiation (λ = 1.54056 Å). IR spectra were recorded on PerkinElmer Spectrum One FT-IR infrared spectrophotometer with pressed KBr pellets in the range of 4000-400 cm^{-1}. Thermal analyses were performed in a dynamic air atmosphere with a heating rate of 10 ºC/min, using a NETZSCH STA 449C thermal analyzer. UV-vis spectra were performed on a SHIMADZU UV-2600 UV-visible spectrophotometer by using the same solvent as the blank.

Adsorption Analysis: Single-component gas measurements were performed with an Accelerated Surface Area and Porosimetry 2020 (ASAP 2020) surface area analyzer. All gases were used in the adsorption experiment of 99.999% purity or higher. The samples of **1-Ln** (300 mg) were activated by degassed under high vacuum at 333 K for 8 h to obtain the evacuated samples.

Ionic conductivity experiments: Ac impedance measurements were carried out with a zennium/IM6 impedance analyzer over the frequency range from 0.1 Hz to 5 MHz with an applied voltage of 50mV. The relative humidity was controlled by a STIK Corp. CIHI-150B incubator. The sample was pressed to form a cylindrical pellet of crystalline powder sample (~1.5 mm thickness ×5 mm φ) coated with Cpressed electrodes. Two silver electrodes were attached to both sides of pellet to form four end S3 terminals (quasi-four-probe method). The bulk conductivity was estimated by semicircle fittings of Nyquist plots.

Synthesis of $H_9[La_9W_8(\mu_4\text{-}O)_{12}(\mu_2\text{-}O)_{24}(H_2O)_{24}](SiW_{12}O_{40})_3\cdot60H_2O$ (1-La): $LaCl_3\cdot6H_2O$ (0.64 mmol, 220 mg), $Na_{10}[\alpha\text{-}SiW_9O_{34}]\cdot16H_2O$ (0.11 mmol, 300 mg), $In(NO_3)_3\cdot4.5H_2O$ (0.52 mmol, 200 mg) and H_5IO_6 (0.65 mmol, 150 mg) were dissolved in 4 mL H_2O in a 20 mL vial, and then the mixture was heated to 100 °C for 4 days and cooled to room temperature. The pH values before and after the reaction were 2.0 and 1.8, respectively. White cube crystals of **1-La** suitable for X-ray diffraction experiments were obtained by filtration, washed with H_2O and air-dried. Yield: about

42.3 % (based on LaCl$_3$·6H$_2$O). Elemental analysis (%) calcd for H$_{177}$Si$_3$La$_9$W$_{44}$O$_{240}$ (13441.63): W, 60.18; La, 9.30; Si, 0.63; Found: W, 59.54; La, 10.06; Si, 0.85. IR (KBr pellet, v/cm^{-1}): 3270(vs), 1635(s), 1000(w), 947(w), 876(w), 675(w), 506(m).

Synthesis of H$_9$[Pr$_9$W$_8$(μ$_4$-O)$_{12}$(μ$_2$-O)$_{24}$(H$_2$O)$_{24}$](SiW$_{12}$O$_{40}$)$_3$·60H$_2$O (1-Pr): The reaction process of **1-Pr** is similar to **1-La** except that PrCl$_3$·6H$_2$O (0.84 mmol, 300 mg) was used to replace LaCl$_3$·6H$_2$O (0.22 mmol, 100 mg). The pH values before and after the reaction were 2.0 and 1.8, respectively. Light green cube crystals of **1-Pr** suitable for X-ray diffraction experiments were obtained by filtration, washed with H$_2$O and air-dried. Yield: 36.5 % (based on PrCl$_3$·6H$_2$O). Elemental analysis (%) calcd for H$_{177}$Si$_3$Pr$_9$W$_{44}$O$_{240}$ (13459.64): W, 60.10; Pr, 9.42; Si, 0.63; Found: W, 58.87; Pr, 9.01; Si, 0.52. IR:3257(vs), 1622(vs), 993(w), 947(w), 882(w), 676(w), 500(w).

Synthesis of H$_9$[Nd$_9$W$_8$(μ$_4$-O)$_{12}$(μ$_2$-O)$_{24}$(H$_2$O)$_{24}$](SiW$_{12}$O$_{40}$)$_3$·60H$_2$O (1-Nd): The reaction process of **1-Nd** is similar to **1-La** except that NdCl$_3$·6H$_2$O (0.75 mmol, 270 mg) was used to replace LaCl$_3$·6H$_2$O (0.22 mmol, 100 mg). The pH values before and after the reaction were 2.0 and 1.8, respectively. Light purple cube crystals of **1-Nd** suitable for X-ray diffraction experiments were obtained by filtration, washed with H$_2$O and air-dried. Yield: 28.9 % (based on NdCl$_3$·6H$_2$O). Elemental analysis (%) calcd for H$_{177}$Si$_3$Nd$_9$W$_{44}$O$_{240}$ (13489.65): W, 59.96; Nd, 9.62; Si, 0.62; Found: W, 58.12; Nd, 8.89; Si, 0.50. IR: 3283(vs), 1623(vs), 1012(w), 954(w), 876(w), 636(w), 513(w).

Single-crystal structure analysis: Single-crystal X-ray diffraction data of **1-La** was collected on Bruker Apex Duo CCD diffractometer with a graphite-monochromatized Mo Kα radiation ($λ$ = 0.71073 Å) operating at 175 K. The structures of **1-La** was solved through direct methods and refined by full-matrix least-squares refinements based on F^2 adopting the SHELX-2014 program package. The contribution of disordered solvent molecules to the overall intensity data of structures were treated using the SQUEEZE method in PLATON. The W(2) ions in **1-La** were disordered and split over two positions. All non-H atoms were located with successive difference Fourier syntheses and refined anisotropically. The H atoms of the free water molecules and coordinated water molecule have not been included in the final refinement.

Crystallographic data and structure refinements for **1-La** is summarized in Table S1. CCDC 1967584 contains supplementary crystallographic data for this paper. These data can be obtained free of charge from The Cambridge Crystallographic Data Centre via www.ccdc.cam.ac.uk/data_request/cif.

Solvent stability test: The crystals of **1-La** (30 mg) were soaked in different solvents (5 mL CH_2Cl_2 = dichloromethane, CH_3CN = acetonitrile, CH_3COCH_3 = acetone, CH_3OH = methanol, EtOH = ethanol, DMF = N,N'-dimethylformamide, NMF = N-Methylformamide) for 24 hours. Then, the crystals were filtered, dried at ambient temperature and grinded for PXRD measurements.

Dye adsorption: Freshly prepared **1-La** (50 mg) were added into to aqueous solutions (5 mL) containing rhodamine B (RhB) (2.0×10^{-5} mol/dm^3), methylene blue (MB) (2.0×10^{-5} mol/dm^3), crystal violet (CV) (2.0×10^{-5} mol/dm^3) and methyl orange (MO) (6.0×10^{-5} mol/dm^3) on 20 mL sealed glass in the dark at room temperature, respectively. UV/Vis spectra were employed to measure the adsorption ability of **1-La** after certain time intervals.

Dye separation: **Freshly** prepared **1-La** (80 mg) were added into to aqueous solutions (5 mL) containing RhB & MB (concentration ratio: 1:1) and MB & MO (concentration ratio: 1:3) on 20 mL sealed glass in the dark at room temperature. The UV/Vis spectra and photographs were employed to measure the selective adsorption abilities of **1-La** after certain time intervals.

The following equations are used to calculate the adsorption efficiency and the quantity:

$$dye\ removal(\%) = \frac{C_0 - C_t}{C_0} \times 100$$

$$Q(quantity) = \frac{C_0 - C_t}{m} \times V \times M$$

In which C_0 is the initial concentration of dye solution and the C_t represents the concentration of **1-La** that adsorbs the dyes at t min, V is the volume of the solution (L), m and M are the mass of adsorbent **1-La** and the molar mass of dyes, respectively.

Section S2 Additional Table

Table S1 Crystal Data and Structure Refinement for **1-La**

	1-La
Empirical formula	$La_9O_{240}Si_3W_{44}H_{129}$
Formula weight	13393.88
Crystal system	Cubic
Space group	$Fm\overline{3}c$ ((#. 226)
a (Å)	37.5612(3)
b (Å)	37.5612(3)
c (Å)	37.5612(3)
V (Å³)	52993.0(13)
Z	8
F(000)	46880
crystal size / mm³	0.26 × 0.25 × 0.24
ϑ range / °	2.425 to 25.031
limiting indices	$-32 \leq h \leq 44$
	$-43 \leq k \leq 41$
	$-35 \leq l \leq 42$
ρ_{calcd}(g cm^{-3})	3.358
Temperature (K)	175(2)
$\mu(mm^{-1})$	20.543
Refl. Collected	38112
Independent relf.	2067
Parameters	112
R_{int}	0.0337
GOF on F²	1.099
Final R indices ($I= 2\sigma(I)$)	$R_1= 0.0319$, $wR_2= 0.0900$
R indices (all data)	$R_1= 0.0346$, $wR_2= 0.0916$

[a]$R_1 = \Sigma||F_o| - |F_c||/\Sigma|F_o|$, [b]$wR_2 = [\Sigma w(F_o^2 - F_c^2)^2/w(F_o)^2]^{1/2}$, $w = 1/[\sigma^2(F_o^2) + (xP)^2 + yP]$, $P = (F_o^2 + 2F_c^2)/3$

Table S2 A summary of known vapor adsorption capacities of polyoxometalate materials

Compounds	Amount (cm^3g^{-1})	Ref.
1-La	124.98	This work
1-Pr	114.79	This work
1-Nd	109.80	This work
$K_3[Cr_3O(OOCH)_6(H_2O)_3][R-SiW_{12}O_{40}]$	130	S2
$Cu_6(Trz)_{10}(H_2O)_4[H_2SiW_{12}O_{40}]\cdot8H_2O$	118	S3
$[Cu_4(dpdo)_{12}][H(H_2O)_{27}(CH_3CN)_{12}][PW_{12}O_{40}]_3$	65.1	S4
$K_2[Cr_3O(OOCH)_6(mepy)_3]_2[\alpha-PMo_{12}O_{40}]\cdot5H_2O$	56.8	S5
$H_{14}[Na_6(H_2O)_{12}]_4[K_{42}Ge_8W_{72}O_{272}(H_2O)_{60}]\cdot solvent$	52	S6
$[Cu_3(L)_2(H_2O)_4][Cu(dmf)_4(SiW_{12}O_{40})]\cdot9H_2O$	51.7	S7
$H[Ni(Hbpdc)(H2O)_2]_2[PW_{12}O_{40}]\cdot8H_2O\}$	31	S8
$[Co(pn)_3]_4[PNb_{12}O_{40}(VO)_6][OH]_5\cdot20H_2O$	19.72	S9
$(DODA)_{23}[Mo_{154}O_{462}H_5]\cdot70H_2O$	16.6	S10
$Cs_{3.6}K_{0.4}[PW_{11}O_{39}(Sn-OH)]\cdot8H_2O$	0.31	S11
$K_2[Cr_3O(OOCH)_6(mepy)_3]_2[a-SiW_{12}O_{40}]\cdot2H_2O\cdot CH_3OH$	0.03	S12
$Cs_2[Cr_3O(OOCC_2H_5)_6(H_2O)_3]_2[R-SiW_{12}O_{40}]\cdot4H_2O$	0.022	S13, S14
$Cs_3H_{0.3}[SiW_{12}O_{40}]_{0.83}\cdot3H_2O$	0.020	S15

Trz: 1,2,4-triazole; dpdo: 4,4'-bipyridine-N,N'-dioxide; mepy: 4-methylpyridine; L: *N,N*-bis[(2-hydroxy-3-methoxyphenyl) methylidene] hydrazine hydrate; dmf：N,N-Dimethylformamide; H₂bpdc: 2,2'-bipyridyl-3,3'-dicarboxylicacid; pn: 1,2-diaminopropane; DODA: dimethyldioctadecylammonium.

Section S3 Additional Figures
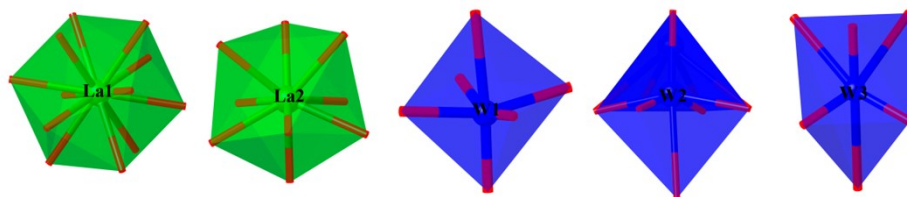
Fig. S1. View of the coordination environments of La^{3+} and W^{6+} ions in **1-La**.
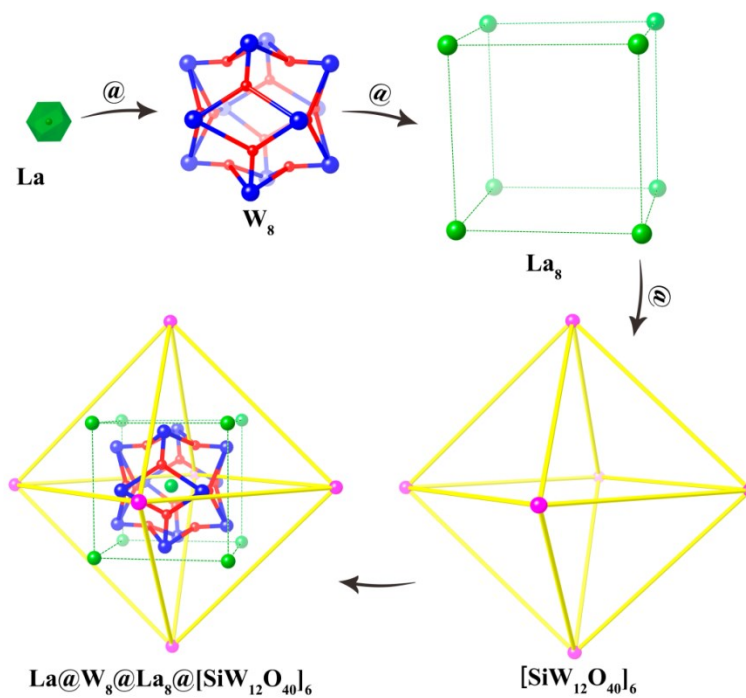
Fig. S2. View of the geometric arrangements of a La^{3+} ion, 8 W^{3+} ions, 8 La^{3+} ions and 6 {SiW$_{12}$O$_{40}$}$^{4-}$ cluster in the four-shell structure, respectively.
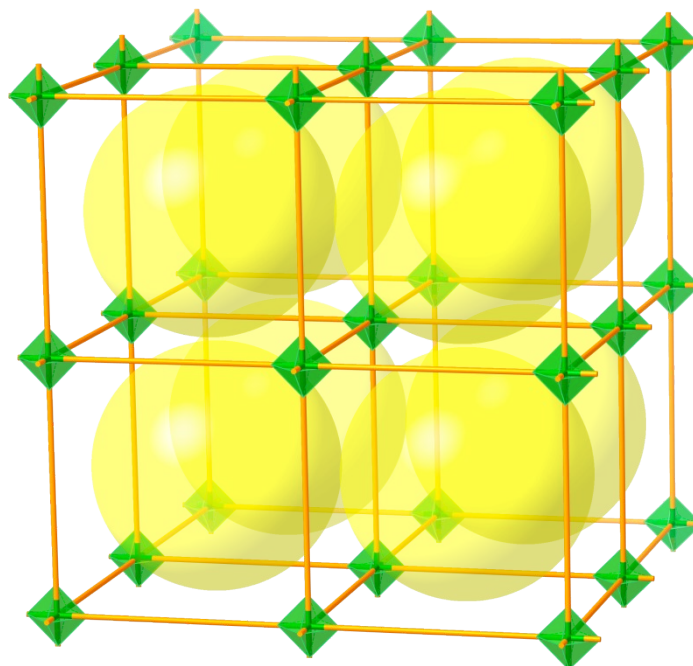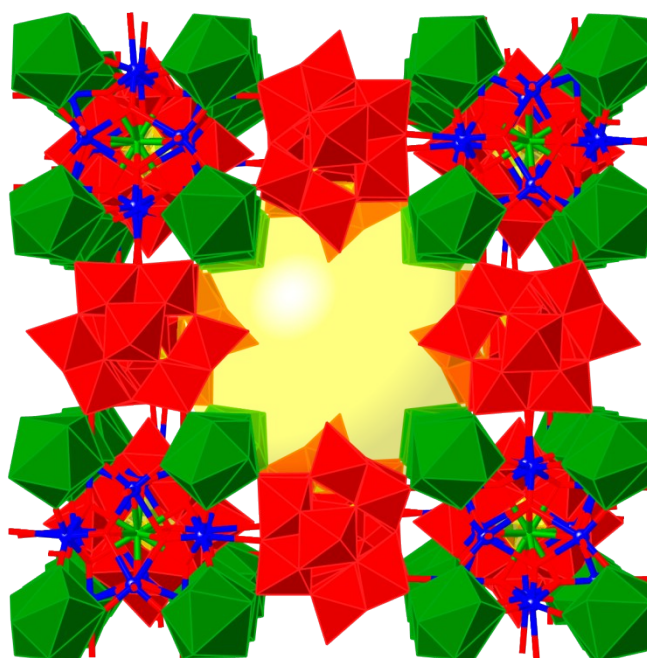
Fig. S3. The topology of **1-La**.

Fig. S4. The cubic-type cage made up of La@W_8@La_8 clusters as vertices and {$SiW_{12}O_{40}$}

clusters as edges.
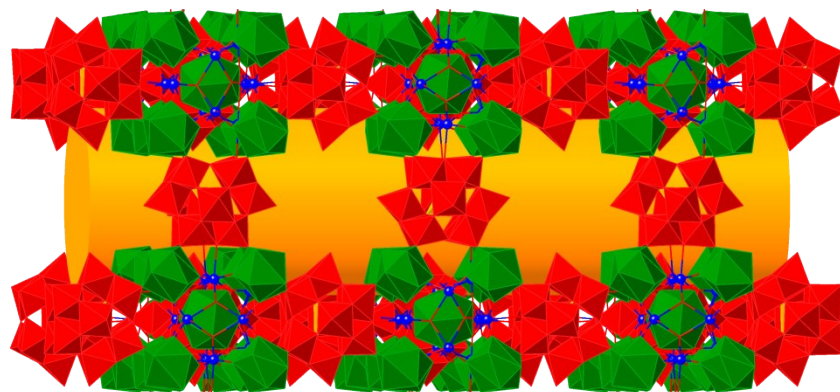
Fig. S5. The square channels of ~1.1 × 1.1 nm^2 along the *a/b/c* axis.
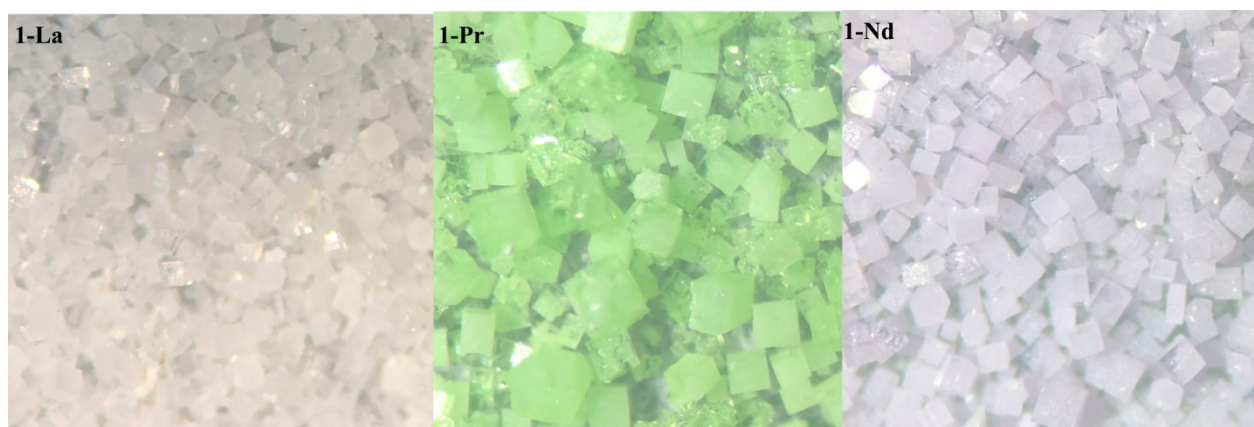
Fig. S6. Crystal morphology of **1-Ln** under an optical microscope.
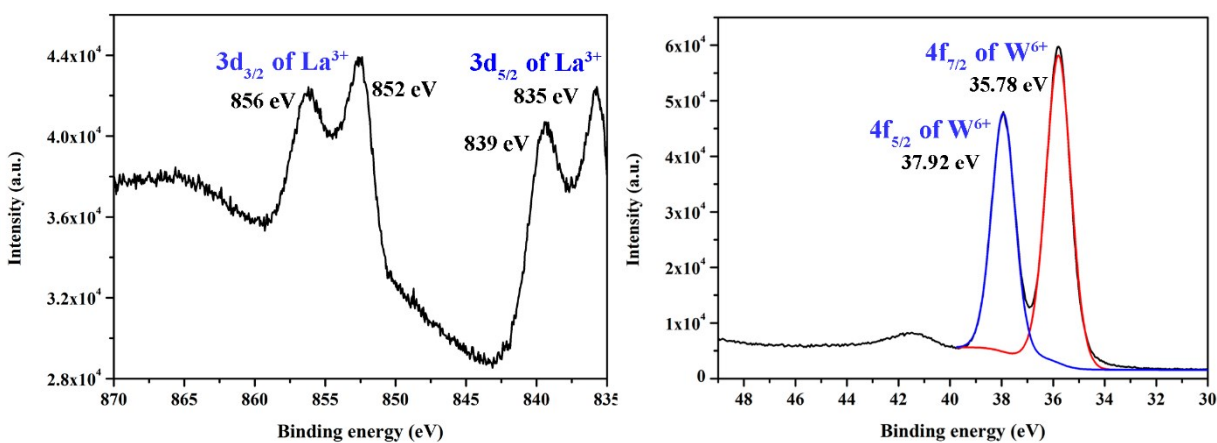
Fig. S7. X-ray photoelectron spectroscopy of the La (3d) and W (4f).
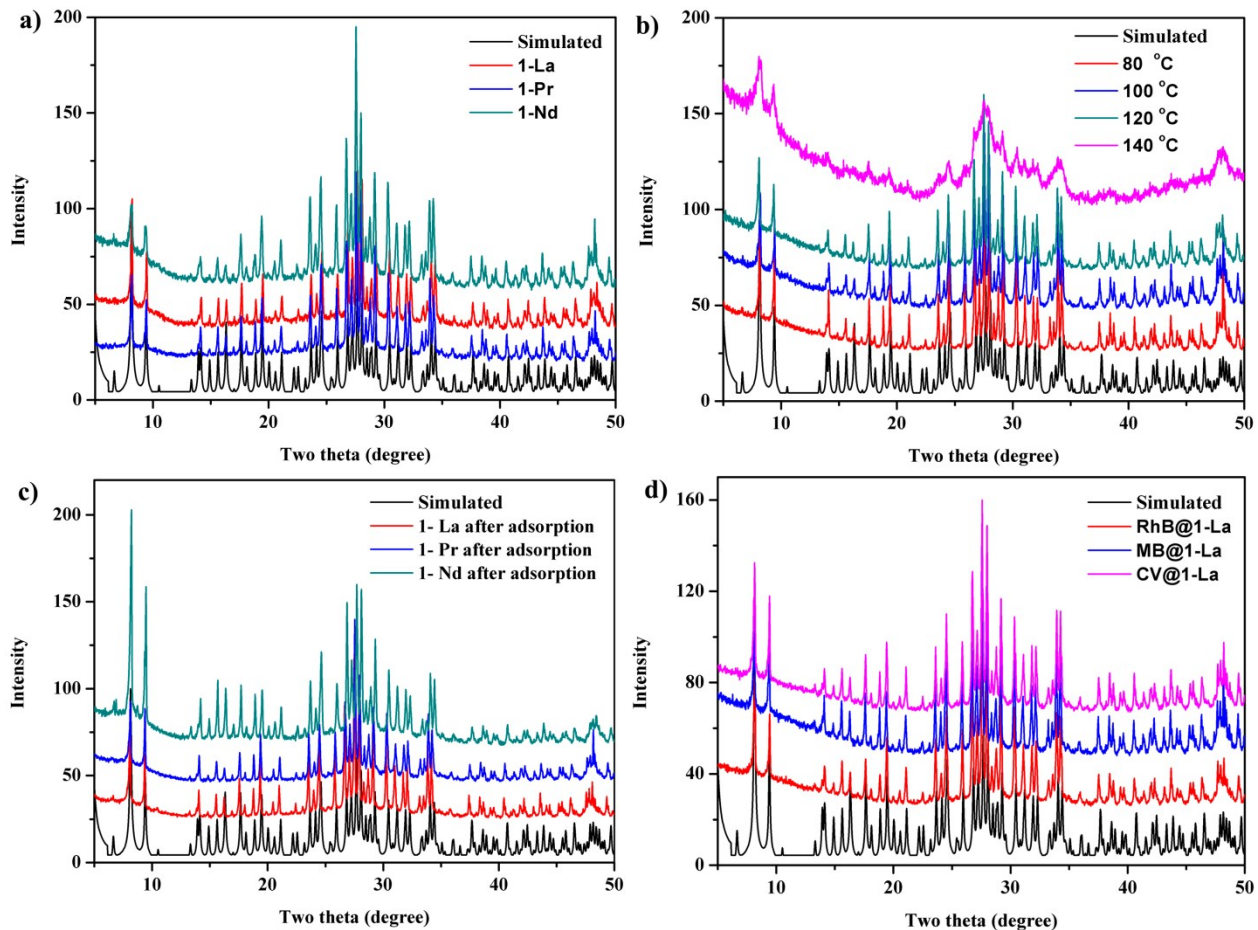
Fig. S8. The simulated and experimental PXRD patterns of **1-Ln**.
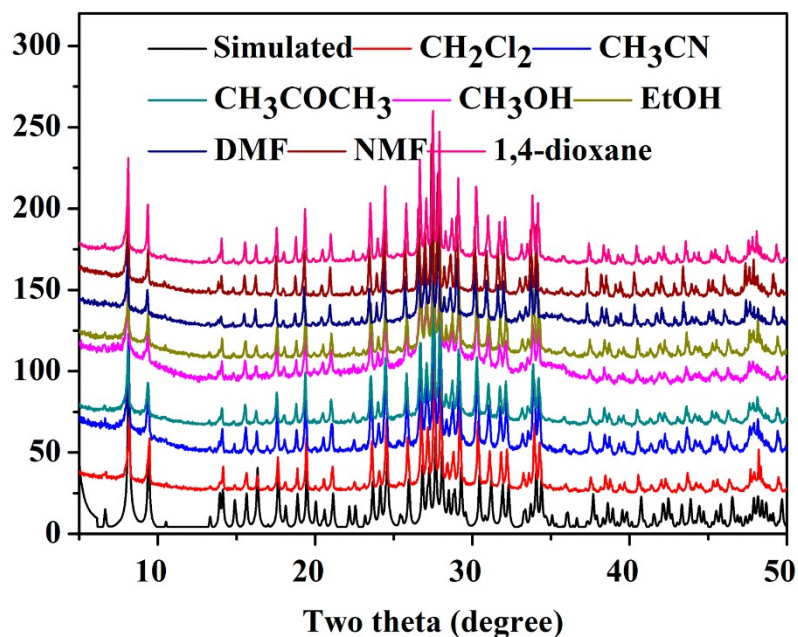
Fig. S9. PXRD patterns of **1-La** after being soaked different organic solvent.
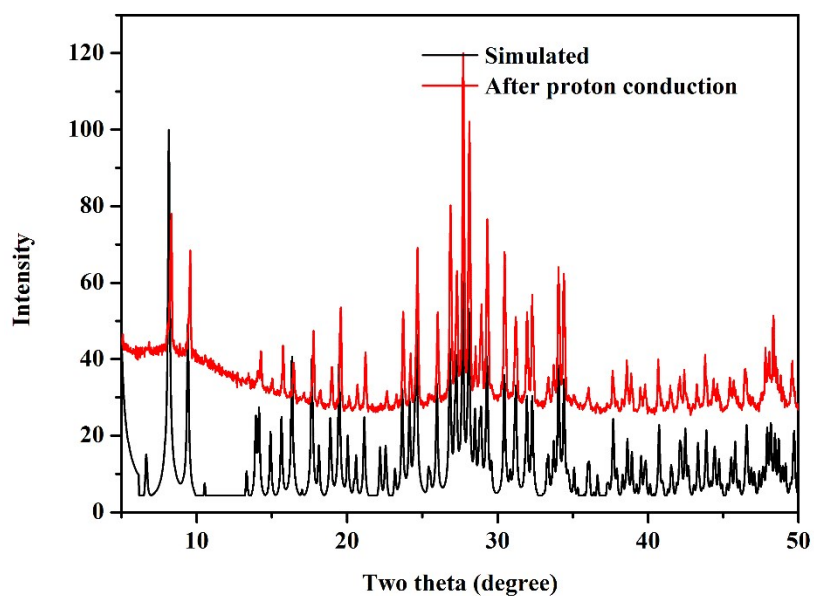
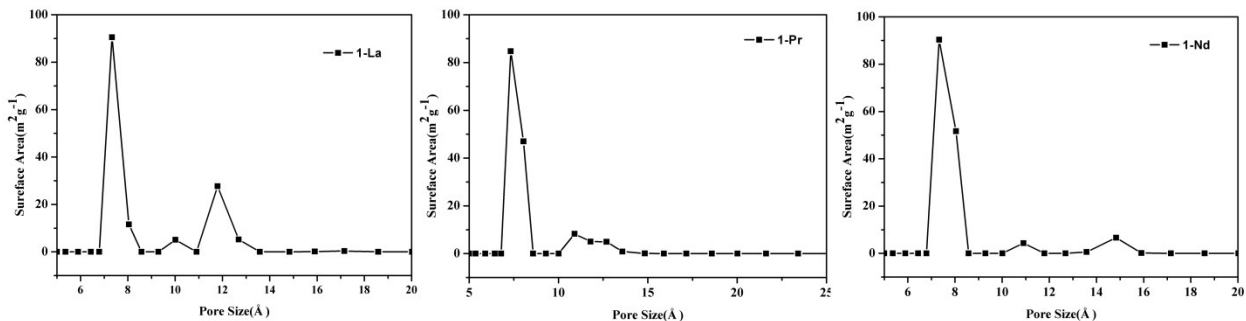**Fig. S10**. PXRD patter after proton conduction for **1-La**.
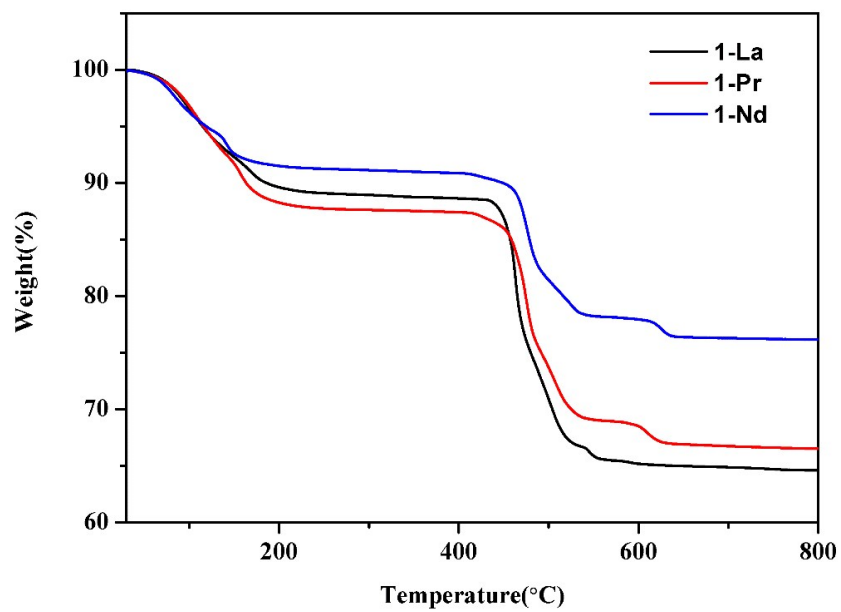
Fig. S11. TG curves of **1-Ln**.

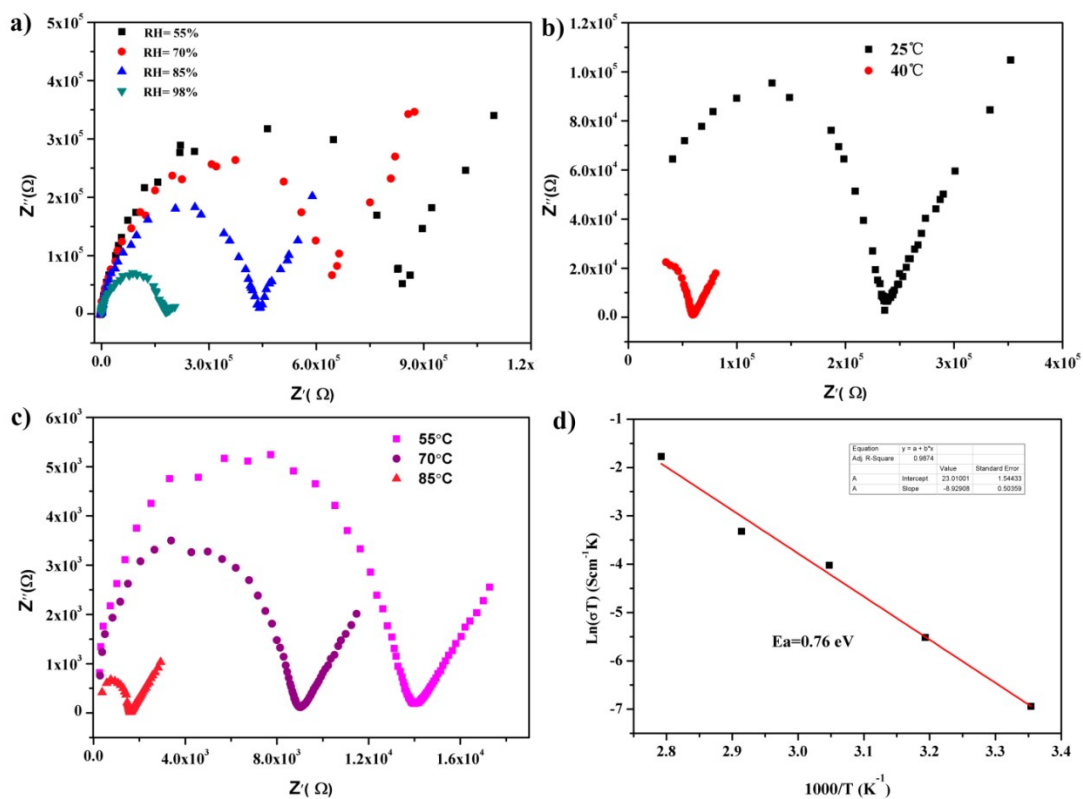**Fig. S12**. The pore size distributions of **1-Ln**.

Fig. S13 a) Nyquist plots for **1-La** at different relative humidity (RH) and *T* = 25 ºC. b) and c) Nyquist plots for **1-La** at different temperature and 98 % RH. d) Arrhenius plots of the conductivity of **1-La**.
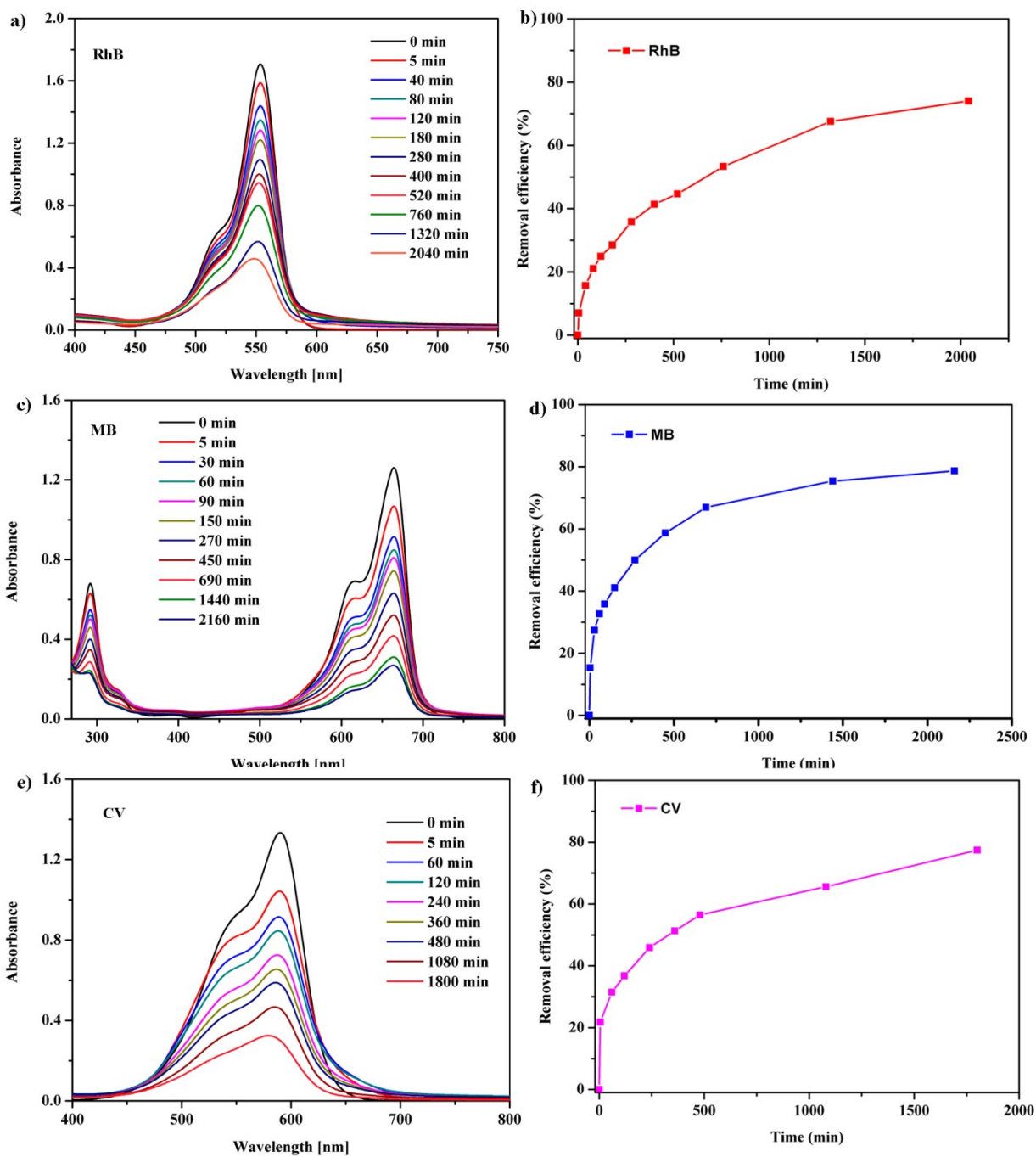
Fig. S14. UV/vis absorption spectra for a) RhB, c) MB and e) CV adsorption by 50 mg of **1-La** in 5 mL of aqueous solutions of dye. b) RhB, d) MB and f) CV its removal efficiency with time.
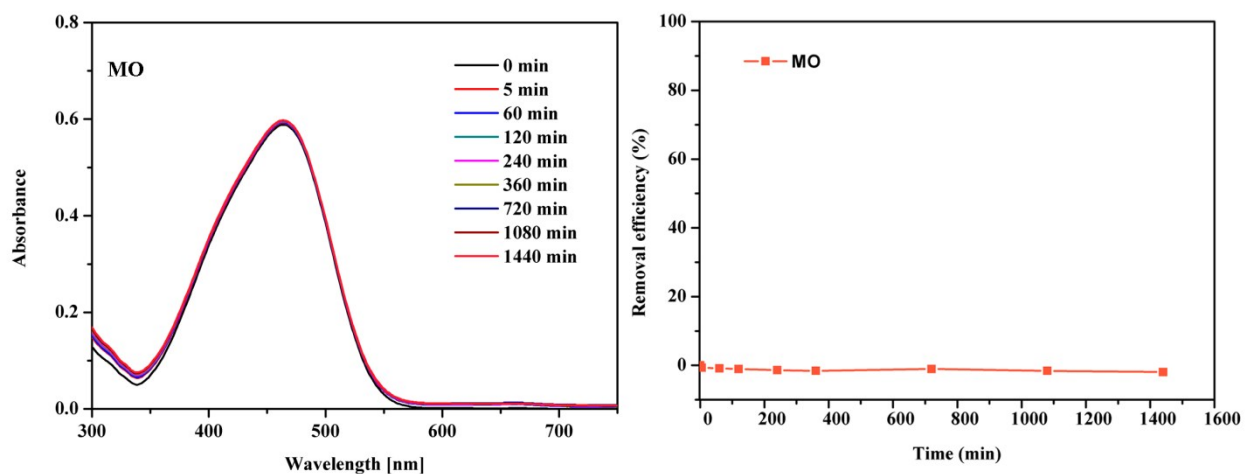
Fig. S15. UV/vis absorption spectra for a) MO adsorption by 50 mg of **1-La** in 5 mL of aqueous solutions of dye. b) its removal efficiency with time.
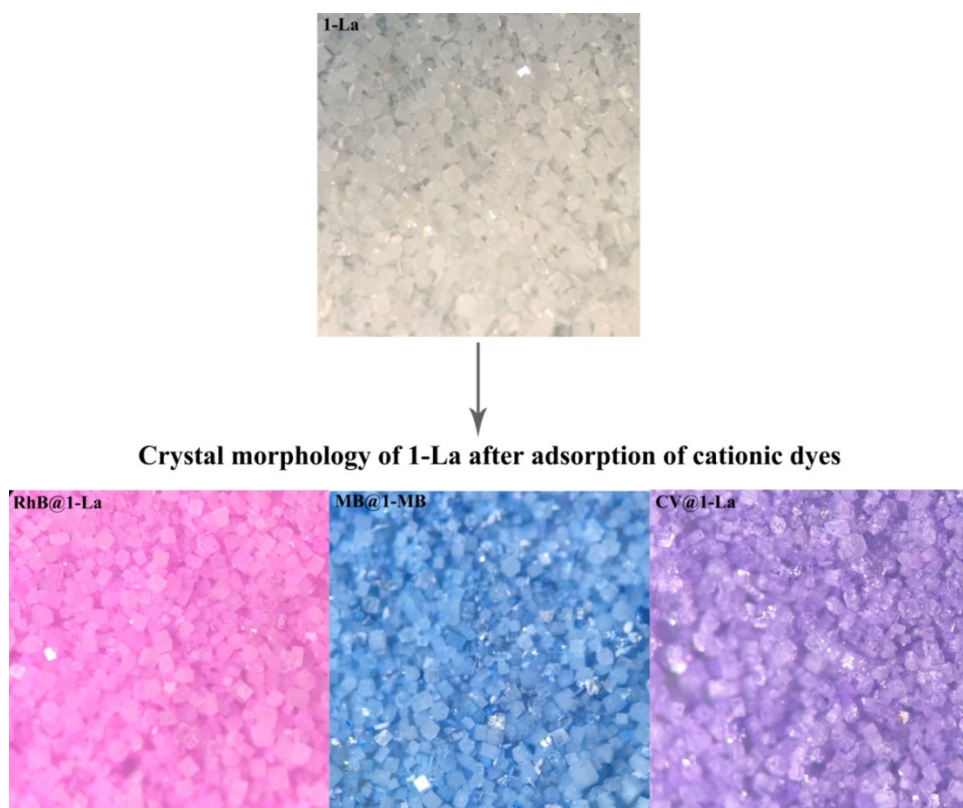

Fig. S16. Crystal morphology of **1-La** after dye adsorption under optical microscope.
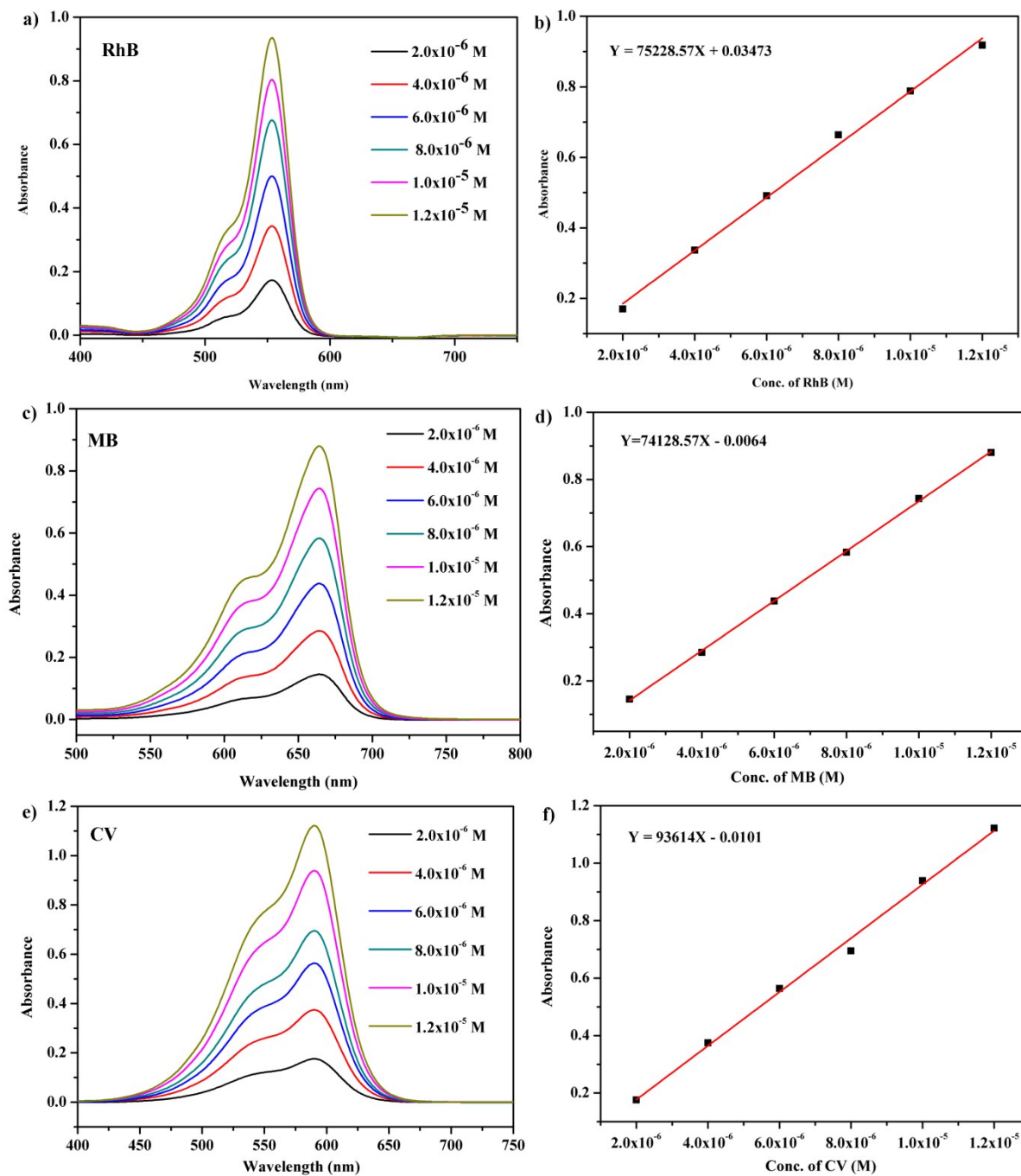
Fig. S17. Calibration plots of standard RhB, MB and CV (a & c & e) by UV-Vis spectra in aqueous solutions and their fitting of Abs. vs concentration of respective dye values (b & d & f).
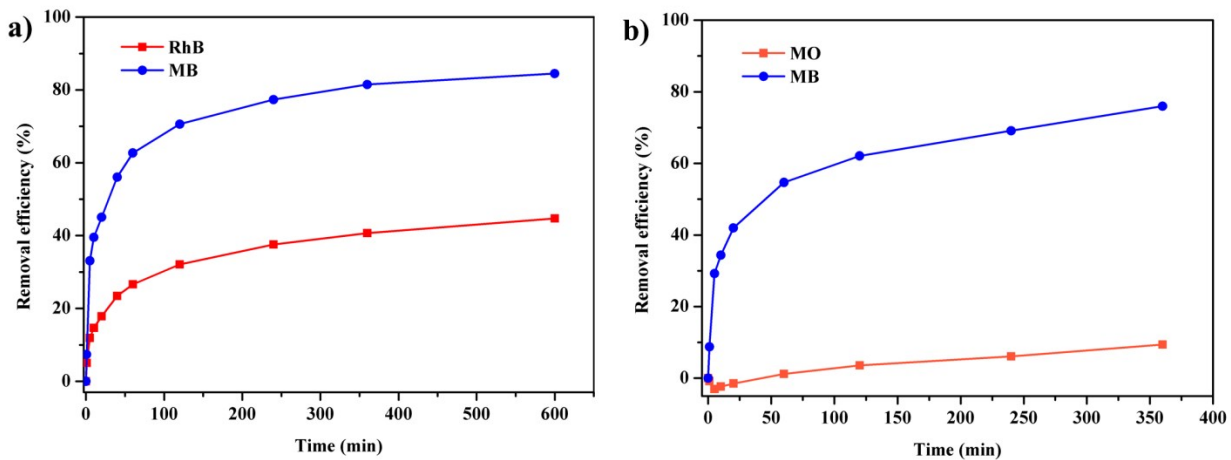
Fig. S18. The removal efficiency of **1-La** versus time in solution of mixed dyes, a) RhB & MB. b) MO & MB.

Section S4 References

S1 A. Tézé, G. Hervé, R. G. Finke, D. K. Lyon, *Inorg. Synth.* 1990, **27**, 85-135.

S2 S. Uchida, R. Kawamoto, N. Mizuno, *Inorg. Chem.* 2006, **45**, 5136-5144.

S3 E. L. Zhou, C. Qin, P. Huang, X. L. Wang, W. C. Chen, K. Z. Shao, Z. M. Su, *Chem. Eur. J.* 2015, **21**, 11894-11898.

S4 M. Wei, L. Chen, X. Duan, J. *Coord. Chem.* 2014, **67**, 2809-2819.

S5 R. Kawahara, S. Uchida, N. Mizuno, *Chem. Mater.* 2015, **27**, 2092-2099.

S6 Z. Li, L. D. Lin, H. Yu, X. X. Li, S. T. Zheng, *Angew. Chem. Int. Ed.* 2018, **57**, 15777-15781.

S7 M. L. Wei, J. J. Sun, X. Y. Duan, *Eur. J. Inorg. Chem.* 2014, 345-351.

S8 M. Wei, X. Wang, J. Sun, X. Duan, *J. Solid State Chem.* 2013, **202**, 200-206.

S9 J. Hu, Y. Xu, D. Zhang, B. Chen, Z. Lin, C. Hu, *Inorg. Chem.* 2017, **56**, 10844-10847.

S10 S. Noro, R. Tsunashima, Y. Kamiya, K. Uemura, H. Kita, L. Cronin, T. Akutagawa, T. Nakamura, Angew. Chem. Int. Ed. 2009, 48, 8703-8706; *Angew. Chem.* 2009, **121**, 8859-8862.

S11 Y. Miura, H. Imai, T. Yokoi, T. Tastumi, Y. Kamiya, *Microporous Mesoporous Mater.* 2013, **174**, 34-43.

S12 S. Uchida, R. Eguchi, N. Mizuno, *Angew. Chem. Int. Ed.* 2010, **49**, 9930-9934; *Angew. Chem.* 2010, **122**, 10126-10130.

S13 A. Lesbani, R. Kawamoto, S. Uchida, N. Mizuno, *Inorg. Chem.* 2008, **47**, 3349-3357.

S14 C. Jiang, A. Lesbani, R. Kawamoto, S. Uchida, N. Mizuno, *J. Am. Chem. Soc.* 2006, **128**, 14240-14241.

S15 Y. Ogasawara, S. Uchida, T. Maruichi, R. Ishikawa, N. Shibata, Y. Ikuhara, N. Mizuno, *Chem. Mater.* 2013, **25**, 905-911.